UCD School of Mathematics and Statistics

Droplet Impact: Modelling and Applications

Joseph Anderson and Lennon Ó'Náraigh

5th August 2024

***Abstract*— Previous work has successfully modelled water droplet impacts with reasonable accuracy to reality. This work mainly aims to improve the treatment of the contact angle in the newly introduced 3D model. This will be performed using the open source CFD library OpenFOAM which will allow us to simulate the droplet impacts. The contact angle will be measured in experiment and then input into the OpenFOAM simulation in the hope to improve accuracy of the 3D model.**

I. INTRODUCTION

A. Context

Droplet impact research is fueled by its many practical applications. Many of them are related to different processes in manufacturing such as ink-jet printing and crop spraying [1]. They also have uses in forensic science as the analysis of blood stains could reveal useful information about the previous conditions of a crime scene [2].

This project will build on previous work done by two students. Firstly, Juan Mairal (a former masters student) used OpenFOAM to create a 2D planar simulation of a water droplet impact and compared it to other methods of simulation. He concluded that OpenFOAM had shorter computation times than other methods due to its open-source nature. Following on from this Conor Quigley (a former undergraduate student) constructed a 3D simulation in a wedge. He was then able to compare the model qualitatively with results from an experiment that used a high-speed camera to capture the water droplet impact. However, Conor used a constant contact angle for his simulations due to time limitations for his project.

B. Contact Angles

Consider a water droplet falling onto a flat surface. The contact line is a triple point where the air, water and surface all meet. The contact line plays an important role in the prevailing physics behind a droplet impact. The contact line appears to contradict the usual no-slip condition, as it shifts along the surface during different impact phases [3]. There is still ongoing debate about how to accurately model these contact lines [4]. This work will focus on the contact angle θ.

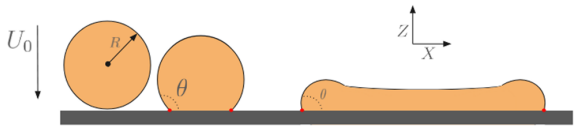

FIG 1: Shows the impact of a water droplet against a hard surface with terminal velocity U_0. The contact line is shown as two dots in the XZ plane (side-view). The contact angle is represented by θ.

II. MATHEMATICAL FRAMEWORK

A. Two-Phase Flow

A water droplet falling in air is an example of a two phase flow where Ω_1 is the air region and Ω_2 is the water region. The surface seperating the two fluids is the interface define as $\phi(x, y, z, t) = 0$. The fluids are assumed to be incompressible and immiscible, with densities ρ_1, ρ_2 and viscosities μ_1, μ_2 respectively.

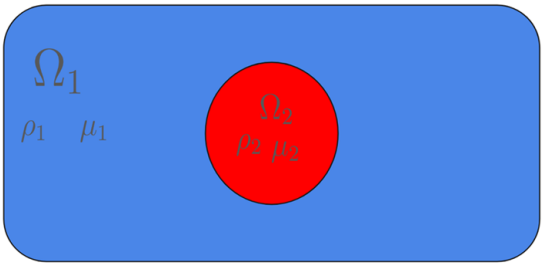

FIG 2: Shows the two-phase flow system that represents the water droplet falling through the air.

This system is governed by the Navier-Stokes equations:

$$\rho_i \frac{D\vec{u_i}}{Dt} = -\vec{\nabla} p_i + \vec{\nabla} \cdot [\mu_i (\vec{\nabla}\vec{u_i} + \vec{\nabla}\vec{u_i}^T)] + \vec{F_{b_i}}, \quad (1)$$

$$\nabla \cdot \vec{u}_i = 0, \quad (2)$$

where $i = 1, 2$ denotes the phase, $\vec{F_{b_i}}$ are the body forces involved and $\frac{D}{Dt}$ is the material derivative defined as $\frac{Df}{Dt} = \frac{\partial f}{\partial t} + \vec{u} \cdot \vec{\nabla} f$. Along the interface ϕ there are continuity conditions that are required. These conditions are the continuity of velocity (Eq. 3), the continuity of tangential stress (Eq. 4) and the jump on the normal stress that is balanced by surface tension (Eq. 5):

$$\nabla [\vec{u}]_\phi = 0, \quad (3)$$

$$\nabla [\hat{n} \cdot \sigma \cdot \hat{t}]_\phi = 0, \quad (4)$$

$$\nabla [\hat{n} \cdot \sigma \cdot \hat{n}]_\phi = -\gamma\kappa, \quad (5)$$

where $\hat{n}$ is the unit normal vector from the interface, $\hat{t}$ is the unit tangential vector from the interface, σ is the stress energy tensor, γ is the surface tensor magnitude, $\kappa = \vec{\nabla} \cdot \hat{n}$ and is the curvature of the interface. The Navier-Stokes equations will give the flow of the fluids. However, to solve for the evolution of the interface we assume that the interface is advected with the flow giving:

$$\left[\frac{D\phi}{Dt}\right]_{\phi=0} = \frac{\partial \phi}{\partial t} + \vec{u} \cdot \vec{\nabla}\phi = 0. \quad (6)$$

B. Volume of Fluid Method

InterFoam is the solver used in OpenFOAM for two-phase flow problems using the Volume of Fluid (VOF) method. It introduces the volume fraction as $\chi(x, y, z)$:

$$\chi(\vec{x}) = \begin{cases} 1 & \text{if } \vec{x} \text{ is in phase 1,} \\ 0 & \text{otherwise.} \end{cases} \quad (7)$$

A smoothed volume fraction $\alpha(x, y, z)$ is also introduced as a measure of how much of phase 1 there is in a discrete volume:

$$\alpha(\vec{x}) = \frac{1}{V} \int_V \chi(\vec{x}')\, d^3\vec{x}'. \quad (8)$$

The global fraction is used to rewrite the global density and global viscosity as a weighted average over the whole domain:

$$\rho(\vec{x}) = \rho_1 \alpha(\vec{x}) + \rho_2 (1 - \alpha(\vec{x})) \quad (9)$$

$$\mu(\vec{x}) = \mu_1 \alpha(\vec{x}) + \mu_2 (1 - \alpha(\vec{x})) \quad (10)$$

These global variables can be used in the Navier-Stokes equations as a set for the whole domain resulting in:

$$\rho \frac{D\vec{u}}{Dt} = -\vec{\nabla} p + \vec{\nabla} \cdot \left[\mu \left(\vec{\nabla}\vec{u} + (\vec{\nabla}\vec{u})^T\right)\right] - \rho \vec{g}\hat{z} + \vec{F}_{st}, \quad (11)$$

$$\nabla \cdot \vec{u} = 0, \quad (12)$$

where $\vec{F}_{st}$ is the force due to surface tension. This is particularly hard to calculate as it only acts on the interface. In the VOF method, the surface tension is formulated as a continuous body force which acts upon the whole domain, this force is zero everywhere except along the interface. Using Brackbill's continuum method for modeling surface tension [5] it can be derived that:

$$\vec{F}_{ST} = \pm\gamma \vec{\nabla} \left(\vec{\nabla} \cdot \left[\frac{\vec{\nabla}\alpha}{|\vec{\nabla}\alpha|} \right] \right), \quad (13)$$

where $\left[\frac{\vec{\nabla}\alpha}{|\vec{\nabla}\alpha|}\right] = \cos\theta$ with θ being the contact angle. To solve the system using VOF, a description of how the interface evolves is also required, this is simple to formulate. Starting from the conservation of mass $\frac{Dm}{Dt} = 0$ where naturally $m = \rho V$, and remembering the two fluids are incompressible, i.e. $\frac{\partial \rho}{\partial t} = 0$ where $\rho_1 \neq \rho_2$, it is shown then that:

$$\frac{D\alpha}{Dt} = 0. \quad (14)$$

The interFoam solver works by numerically solving Eq. 11 and Eq. 14. The treatment of the contact angle, θ, is an important variable. It could be treated as a constant value over time which is how C. Quigley (2024) previously implemented it during his final year project [6]. However, this has its limitations as this is not what is seen in experiments. Instead, the contact angle changes with respect to time. The OpenFOAM implementation of the dynamic contact angle follows:

$$\theta = \theta_e + (\theta_a - \theta_r) \tanh\left(\frac{U_{wall}}{U_\theta}\right), \quad (15)$$

where θ_e is the equilibrium contact angle, θ_a is the advancing contact angle, θ_r is the receding contact angle, U_{wall} is an approximation of the velocity at the contact line and U_θ is a velocity parameter without a clear physical meaning. Thus, the dynamic angle varies between the values $\theta_e \pm (\theta_a - \theta_r)$ with the speed of the variation depending on the choice of U_θ.

III. Experimental Values

We conducted an experiment of a water droplet falling on a hard surface being captured by a high-speed camera. These videos would be used to measure the contact angle over time.

A. Setup

The setup of this experiment was extremely simple consisting of a wooden jig which held a high-speed camera level to a smooth aluminum plate. A wooden strut held a syringe and nozzle which allowed for the careful dropping of single droplets. A light source was held behind the droplet in order to improve the visibility of the droplet. The droplets would fall to the plate where the camera would capture the detail of the impact.

FIG 3: Shows the apparatus setup with the high-speed camera being held level to the aluminum plate.

For our simulation, we set the distance between the nozzle and the aluminium plate to be around 10 cm. This would give the terminal velocity of the droplet to be approximately 1 m/s. The radius of the droplet was also measured to be approximately 3 mm.

B. Edge Finding

An in-built edge detection method was used in Matlab to process each frame of the captured video. The "edge" function was used with a Sobel filter to detect the edge of the droplet. Other image processing techniques such as linear structure dilation and smoothing are used to improve the accuracy of the edge of the water droplet. Only the upper half of the edge is considered as the other half is a reflection of the droplet.

C. Interpolation Method

Now that we have the edge of the water droplet detected, a polynomial can be fitted to it which will allow us to find the contact angle. We considered independently the left and right side of the droplet as we are looking at a 2D slice of the water droplet using the camera. This will allow us to ensure our model is realistic.

The degree of the polynomial being fitted is crucial to the resulting contact angle. Some early test models we created were over fitting the data and putting too much importance on the next data point after the triple point that meets with the surface. To counteract this we iterated over many different values of the polynomial degree and found the polynomial which had the lowest root-mean-square error between the fitted polynomial and the edge points.

The tangents to these fitted curves can be found and the slope of this line is used to obtain the contact angle. This is performed at each frame of the video taken by the high-speed camera of the droplet.

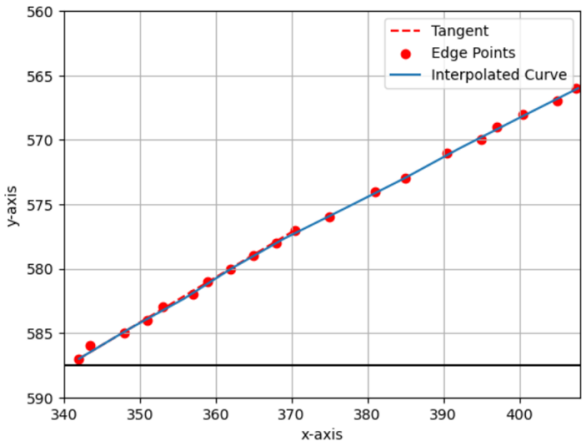

FIG 4: Shows the left side of one of the frames of the droplet impact video with the chosen interpolated curve fitting the edge points from Matlab.

D. Contact Angle

The contact angle can now be calculated on either side of the droplet. The oscillatory motion of the angle can be seen as it settles into its equilibrium value of approximately $\theta_e = 50°$ which was found through averaging angles of the last 20 frames. The advancing and receeding angles can be taken to be $\theta_a = 55°$ and $\theta_r = 45°$, respectively.

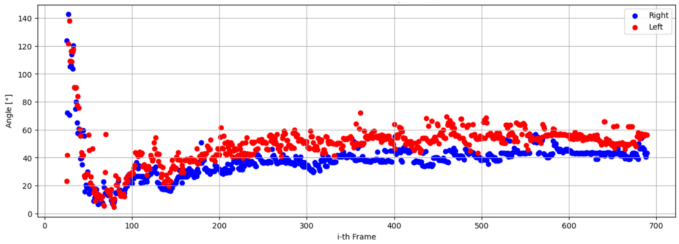

FIG 5: Shows the time series of the contact angle on both sides of the water droplet.

IV. OpenFOAM Simulation

OpenFOAM is a C++ based toolbox which is run through Linux. It is operated by creating scripts which define the domain, initial and boundary conditions and decides which solvers to use.

A. Mesh Generation

The blockMesh defines the simulation domain and splits it into a grid of cubes where Eq. 11 and Eq. 14 are solved. The dimensions of the mesh grid were found by C. Quigley (2024) in order to best capture the important characteristics of the impact whilst minimizing computational time [6]. This created a 3D wedge. The resolution of the grid was defined as $(400\ 1\ 600)$, which means that there is 400 cubes in the x-direction, 1 in the y-direction and 600 in the z-direction. Due to how thin the mesh is in the y direction it was deemed that 1 was a sufficient amount. The thinness of the mesh in this direction was based on the reasoning that most of the flow would be in the radial direction.

The water droplet is defined to have a velocity of $U_0 = (0, 0, 1)$ m/s and radius of 0.003 m. This mimics what was seen in the experiment. The simulation is performed between $t = 0$ and $t = 0.35$ seconds with an adjustable time step allowing the model to save on computational time.

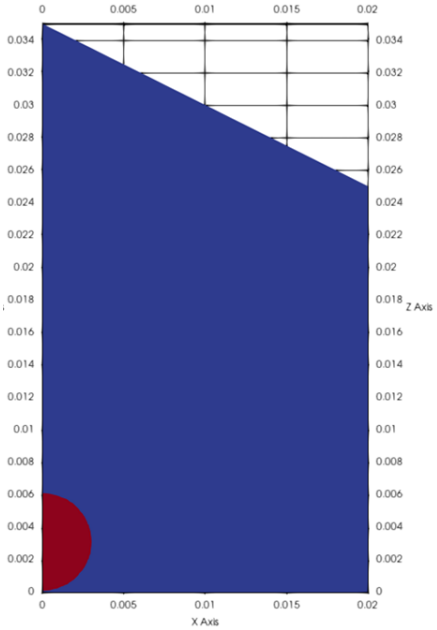

FIG 6: Shows the initialised domain with the droplet in red and the air in blue.

B. Sonic HPC

These simulations can take significant quantities of time to run. In particular, C. Quigley's final simulation took 7 days to run in parallel on 8 laptop cores. We used the Sonic high performance computing cluster in University College Dublin to tackle the simulations. Hence, we could decompose the simulations and run them in parallel on 40 cores which greatly helped computation time. This meant that our simulations ran for 20 hours.

C. Simulations with Discussion

There were 200 time steps saved in intervals of $\tau \approx 0.00175$. These simulations were ran in 3D however, to visualise them we will look at them in 2D. The front of the wedge has been rotated $180°$ leading to the 2D planes shown below.

1) Spreading Phase: The initial impact causes an air bubble to be trapped. In our case the air bubble remains in the center which is as expected [7]. After the impact occurs the spreading phase of the droplet begins to occur shown in Figure 7. This is where the inertial forces of the droplet remain dominant. Hence, the droplet is forced outwards as it thins out until a maximum is reached. During this, the air bubble is released upwards.

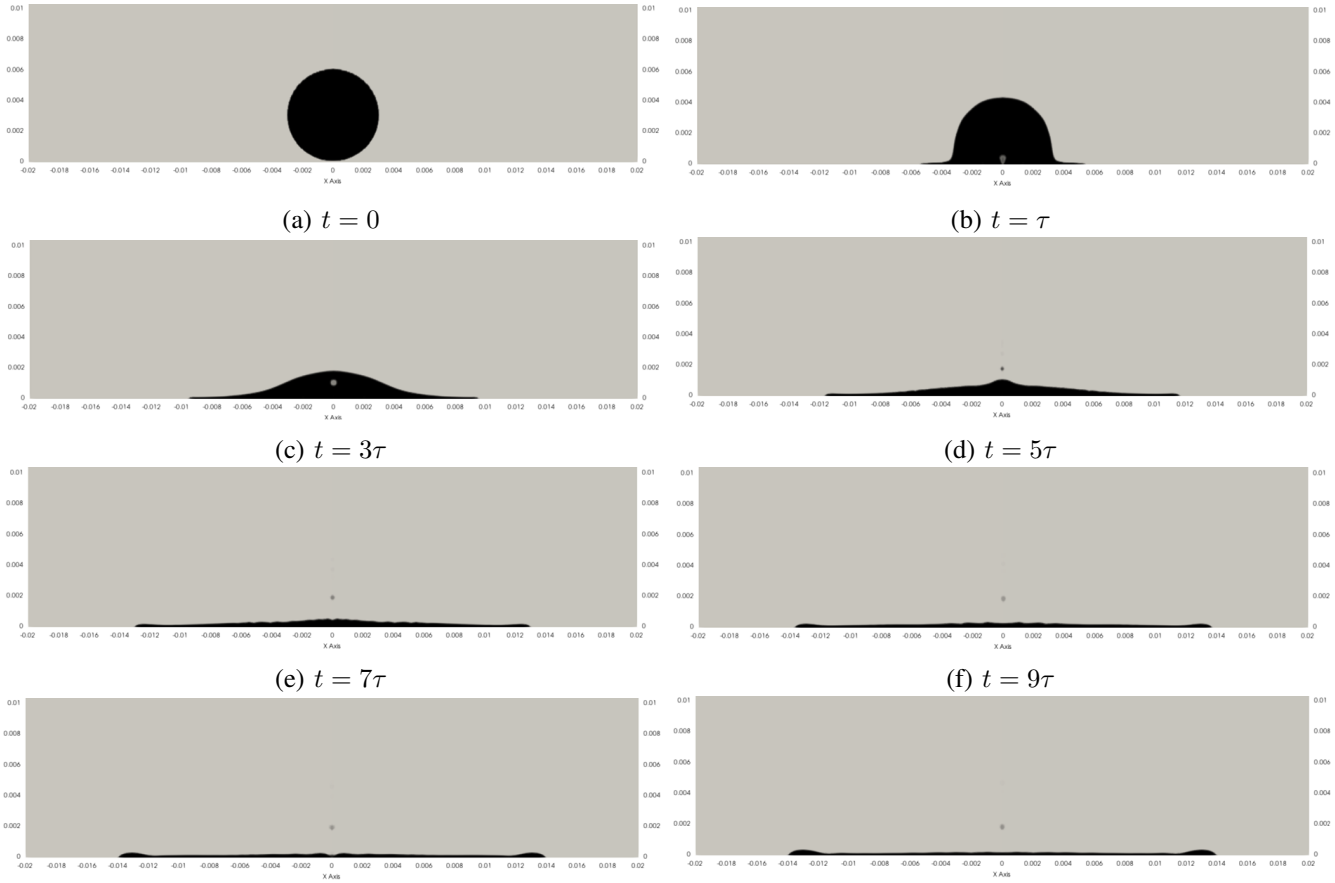

(a) $t = 0$ (b) $t = \tau$

(c) $t = 3\tau$ (d) $t = 5\tau$

(e) $t = 7\tau$ (f) $t = 9\tau$

(g) $t = 11\tau$ (h) $t = 13\tau$

FIG 7: Shows the evolution of the droplet spreading phase starting from the initialisation at $t = 0$. We define $\tau \approx 0.00175$ s.

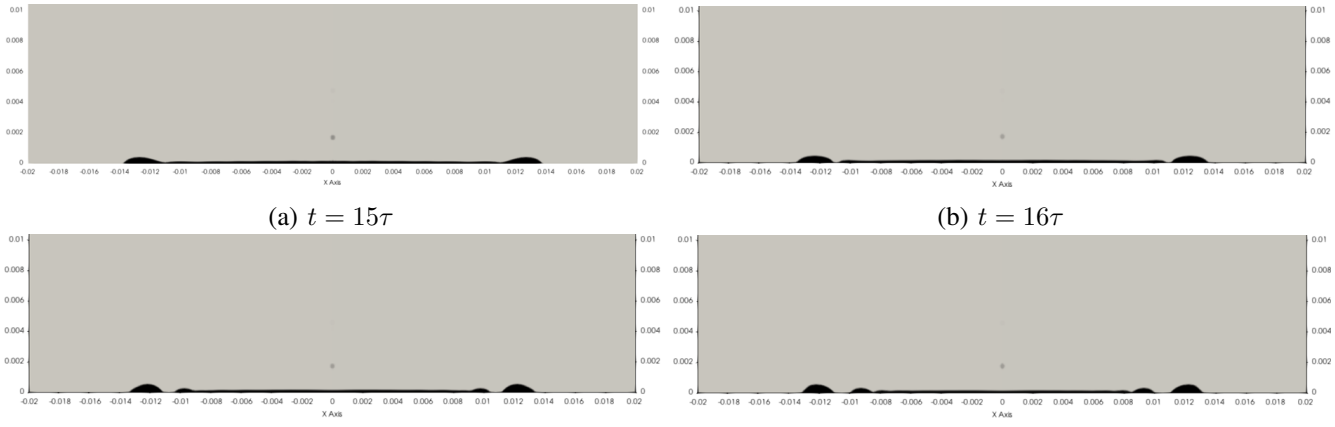

(a) $t = 15\tau$ (b) $t = 16\tau$

(c) $t = 17\tau$ (d) $t = 18\tau$

FIG 8: Shows the break-up of the droplet caused by the thinness of the mesh. The ridge at the edge breaks off from the central lamella.

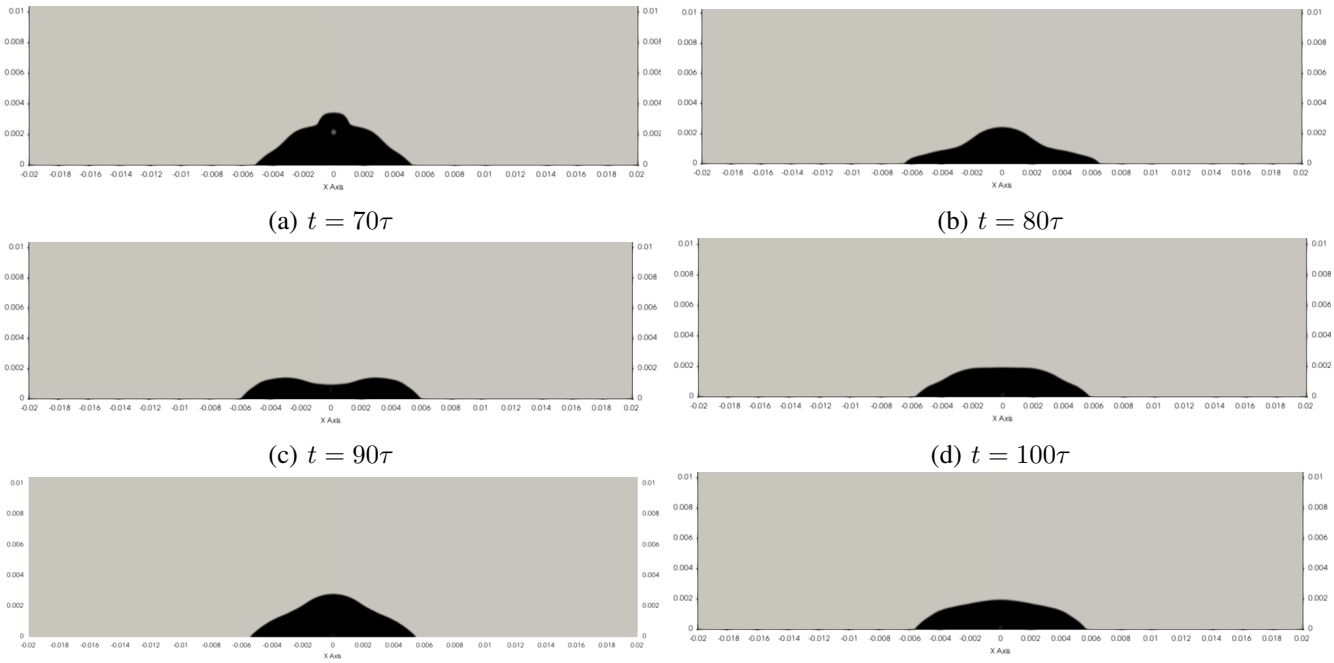

(a) $t = 70\tau$ (b) $t = 80\tau$

(c) $t = 90\tau$ (d) $t = 100\tau$

(e) $t = 110\tau$ (f) $t = 120\tau$

FIG 9: Shows the droplet settling towards its equilibrium state over time where the contact angle is tending towards $\theta_e = 50^\circ$

2) Droplet Break-up: There is then an initial receding phase which is characterised by the nearly equal balance of the inertia of the droplet and the surface tension. The surface tension then begins to dominate causing the creation of the rim on the edge and the flat lamella in the central region. Then, we see the breakup of the droplet where the rim on the edge breaks away from the central lemella which is shown in Figure 8. This seems to be caused by the lamella being so thin that it is comparable with the grid spacing defined by the blockMesh.

3) Equilibrium Phase: The equilibrium phase which was observed towards the end of our simulation is also important. C. Quigley (2024) focused mainly on the earlier parts of the droplet simulation. After the initial phase the droplet forms an upwards jet which then disperses the fluid upwards which he deemed to be nonphysical. In our case the predictive nature of the simulation becomes flawed after the separation of the droplet. However, the latter stages of the simulation still captured some of the essential physics behind the droplet dynamics which is shown in Figure 9. We can see the oscillatory motion of the central part of the droplet as it settles into equilibrium. This behaviour was also observed with the high-speed camera previously. This demonstrates an improvement in the end stage of the simulation compared to what was observed using the constant contact angle model.

D. Parameter Variation

The above simulation was performed using a value of $U_\theta = 6.155$ in Eq. 15. This is the value that was found to give the closest values to the spread ration that would be expected from such a simulation [8]. We also checked the effect that the value of U_θ had on our simulation. We chose a larger ($U_\theta = 18$) and smaller ($U_\theta = 1$) to check its effect. There was no improvement is the realism of the simulation by varying this parameter. The only major difference between the simulations when U_θ was varied was that for the $U_\theta = 1$ case we see a split up of the droplet into three separate parts. This is evident in Figure 10. This breakup is not expected to happen which is why we kept $U_\theta = 6.155$ for our simulations.

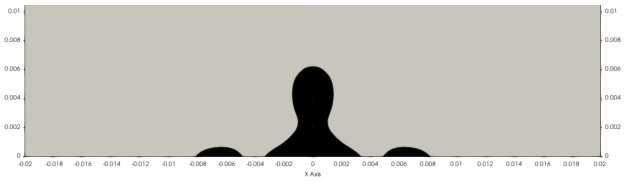

(a) $U_\theta = 6.155$

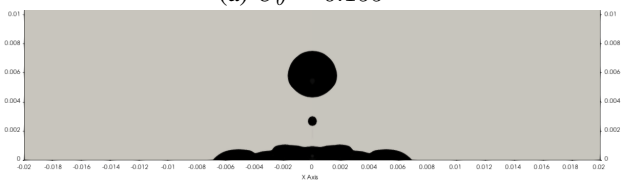

(b) $U_\theta = 1$

FIG 10: Shows the frame for each of the different simulations at $t = 47\tau$.

E. Maximum Spreading

The maximum spreading of the droplet can be found in experiment using the processed images in Matlab. We have previously approximated the droplet radius to be 0.003 m. We can find the maximum spreading of the droplet on the python scale using the frame that has the largest spread. The previous scaling can then be used to find the experimental measurement of 0.018 m.

The maximum spreading of the simulations can be found leading to the values in Table 1. The "Constant θ" simulation refers to the previous 3D implementation of the model using the constant contact angle of $\theta = 90°$. Meanwhile the "Dynamic θ" simulation is our previous simulation where the dynamic contact angle condition is used. We can see that using the dynamic angle model brings the maximum spreading closer to the "true" value found from the experiment.

Version	**Maximum Spreading [m]**
Experiment	0.0180
Constant θ	0.0115
Dynamic θ	0.0140

TABLE I: Maximum spreading values.

V. Conclusion

This study has investigated the effect of using the dynamic contact angle on the 3D simulation of the water impact. We have accurately measured the contact angle over time for a water droplet impact. These values were used to implement the dynamic contact angle model into the 3D OpenFOAM simulation. We have shown the initial spreading phase which matches previous works. The break up of the droplet has been shown due to a numerical error caused by the thinness of the droplet between the outer ridge and the flat lamella. The final stages of our simulation have been shown to more accurately represent the water droplet settling into equilibrium on the surface. The maximum spreading has also been found to be closer to the experimental value by using the dynamic contact angle.

The project has been left in a good place where another student could continue on from. The Sonic cluster will mean that future students will be able to test simulations quicker and easier. Further research could include visualising the flow inside the droplet in order to understand the dynamics within the droplet. A dynamic meshing could be used to try to prevent the numerical error caused by the thin droplet surface. This could lead to an even more realistic model.

Acknowledgements

I would like to thank Lennon Ó'Náraigh for his continued guidance throughout the project. I also want to acknowledge Juan Mairal and Conor Quigley's previous work which helped me greatly.

References

[1] A. L. Yarin, "Drop impact dynamics: splashing, spreading, receding, bouncing…," *Annu. Rev. Fluid Mech.*, vol. 38, no. 1, pp. 159–192, 2006.

[2] D. Attinger, C. Moore, A. Donaldson, A. Jafari, and H. A. Stone, "Fluid dynamics topics in bloodstain pattern analysis: Comparative review and research opportunities," *Forensic science international*, vol. 231, no. 1-3, pp. 375–396, 2013.

[3] S. H. Davis *et al.*, "On the motion of a fluid-fluid interface along a solid surface," *Journal of Fluid Mechanics*, vol. 65, no. 1, pp. 71–95, 1974.

[4] H. Y. Erbil, "The debate on the dependence of apparent contact angles on drop contact area or three-phase contact line: A review," *Surface Science Reports*, vol. 69, no. 4, pp. 325–365, 2014.

[5] J. U. Brackbill, D. B. Kothe, and C. Zemach, "A continuum method for modeling surface tension," *Journal of computational physics*, vol. 100, no. 2, pp. 335–354, 1992.

[6] C. Quigley, "Computational fluid dynamics: 3d openfoam simulation of water droplet impact," Bachelor's thesis, School of Physics, University College Dublin, 2024.

[7] S. Thoroddsen, T. Etoh, K. Takehara, N. Ootsuka, and Y. Hatsuki, "The air bubble entrapped under a drop impacting on a solid surface," *Journal of Fluid Mechanics*, vol. 545, pp. 203–212, 2005.

[8] J. Mairal, "A cross-validation study of computational methods for droplet spreading," Master's thesis, School of Physics, University College Dublin, 2021.